

Making the V in VQA Matter: Elevating the Role of Image Understanding in Visual Question Answering

Yash Goyal^{*1} Tejas Khot^{*1} Douglas Summers-Stay² Dhruv Batra³ Devi Parikh³

¹Virginia Tech ²Army Research Laboratory ³Georgia Institute of Technology

¹{ygoyal, tjskhot}@vt.edu ²douglas.a.summers-stay.civ@mail.mil ³{dbatra, parikh}@gatech.edu

Abstract

Problems at the intersection of vision and language are of significant importance both as challenging research questions and for the rich set of applications they enable. However, inherent structure in our world and bias in our language tend to be a simpler signal for learning than visual modalities, resulting in models that ignore visual information, leading to an inflated sense of their capability.

We propose to counter these language priors for the task of Visual Question Answering (VQA) and make vision (the V in VQA) matter! Specifically, we balance the popular VQA dataset [3] by collecting complementary images such that every question in our balanced dataset is associated with not just a single image, but rather a pair of similar images that result in two different answers to the question. Our dataset is by construction more balanced than the original VQA dataset and has approximately twice the number of image-question pairs. Our complete balanced dataset is publicly available at <http://visualqa.org/> as part of the 2nd iteration of the Visual Question Answering Dataset and Challenge (VQA v2.0).

We further benchmark a number of state-of-art VQA models on our balanced dataset. All models perform significantly worse on our balanced dataset, suggesting that these models have indeed learned to exploit language priors. This finding provides the first concrete empirical evidence for what seems to be a qualitative sense among practitioners.

Finally, our data collection protocol for identifying complementary images enables us to develop a novel interpretable model, which in addition to providing an answer to the given (image, question) pair, also provides a counterexample based explanation. Specifically, it identifies an image that is similar to the original image, but it believes has a different answer to the same question. This can help in building trust for machines among their users.

^{*}The first two authors contributed equally.



Figure 1: Examples from our balanced VQA dataset.

1. Introduction

Language and vision problems such as image captioning [8, 4, 7, 19, 40, 21, 28] and visual question answering (VQA) [3, 26, 27, 10, 31] have gained popularity in recent years as the computer vision research community is progressing beyond “bucketed” recognition and towards solving multi-modal problems.

The complex compositional structure of language makes problems at the intersection of vision and language challenging. But recent works [6, 47, 49, 16, 18, 1] have pointed out that language also provides a strong prior that can result in good superficial performance, without the underlying models truly understanding the visual content.

This phenomenon has been observed in image captioning [6] as well as visual question answering [47, 49, 16, 18, 1]. For instance, in the VQA [3] dataset, the most common sport answer “tennis” is the correct answer for 41% of the questions starting with “What sport is”, and “2” is the correct answer for 39% of the questions starting with “How many”. Moreover, Zhang *et al.* [47] points out a particular ‘visual priming bias’ in the VQA dataset – specifically, subjects saw an image while asking questions about it. Thus, people only ask the question “Is there a clock tower in the picture?” on images actually containing clock towers. As one particularly perverse example – for questions

in the VQA dataset starting with the n-gram “Do you see a ...”, blindly answering “yes” without reading the rest of the question or looking at the associated image results in a VQA accuracy of 87%!

These language priors can give a false impression that machines are making progress towards the goal of understanding images correctly when they are only exploiting language priors to achieve high accuracy. This can hinder progress in pushing state of art in the computer vision aspects of multi-modal AI [39, 47].

In this work, we propose to counter these language biases and elevate the role of image understanding in VQA. In order to accomplish this goal, we collect a balanced VQA dataset with significantly reduced language biases. Specifically, we create a balanced VQA dataset in the following way – given an (image, question, answer) triplet (I, Q, A) from the VQA dataset, we ask a human subject to identify an image I' that is similar to I but results in the answer to the question Q to become A' (which is different from A). Examples from our balanced dataset are shown in Fig. 1. More random examples can be seen in Fig. 2 and on the project website¹.

Our hypothesis is that this balanced dataset will force VQA models to focus on visual information. After all, when a question Q has two different answers (A and A') for two different images (I and I' respectively), the only way to know the right answer is by looking at the image. Language-only models have simply no basis for differentiating between the two cases – (Q, I) and (Q, I') , and by construction must get one wrong. We believe that this construction will also prevent language+vision models from achieving high accuracy by exploiting language priors, enabling VQA evaluation protocols to more accurately reflect progress in image understanding.

Our balanced VQA dataset is also particularly difficult because the picked complementary image I' is close to the original image I in the semantic (fc7) space of VGGNet [37] features. Therefore, VQA models will need to understand the subtle differences between the two images to predict the answers to both the images correctly.

Note that simply ensuring that the answer distribution $P(A)$ is uniform across the dataset would not accomplish the goal of alleviating language biases discussed above. This is because language models exploit the correlation between question n-grams and the answers, *e.g.* questions starting with “Is there a clock” has the answer “yes” 98% of the time, and questions starting with “Is the man standing” has the answer “no” 69% of the time. What we need is not just higher entropy in $P(A)$ across the dataset, but higher entropy in $P(A|Q)$ so that image I must play a role in determining A . This motivates our balancing on a per-question level.

¹<http://visualqa.org/>

Our complete balanced dataset contains approximately *1.1 Million* (image, question) pairs – almost *double* the size of the VQA [3] dataset – with approximately *13 Million* associated answers on the $\sim 200k$ images from COCO [23]. We believe this balanced VQA dataset is a better dataset to benchmark VQA approaches, and is publicly available for download on the project website.

Finally, our data collection protocol enables us to develop a counter-example based explanation modality. We propose a novel model that not only answers questions about images, but also ‘explains’ its answer to an image-question pair by providing “hard negatives” *i.e.*, examples of images that it believes are similar to the image at hand, but it believes have different answers to the question. Such an explanation modality will allow users of the VQA model to establish greater trust in the model and identify its oncoming failures.

Our main contributions are as follows: (1) We balance the existing VQA dataset [3] by collecting complementary images such that almost every question in our balanced dataset is associated with not just a single image, but rather a pair of similar images that result in two different answers to the question. The result is a more balanced VQA dataset, which is also approximately twice the size of the original VQA dataset. (2) We evaluate state-of-art VQA models (with publicly available code) on our balanced dataset, and show that models trained on the existing ‘unbalanced’ VQA dataset perform poorly on our new balanced dataset. This finding confirms our hypothesis that these models have been exploiting language priors in the existing VQA dataset to achieve higher accuracy. (3) Finally, our data collection protocol for identifying complementary scenes enables us to develop a novel interpretable model, which in addition to answering questions about images, also provides a counter-example based explanation – it retrieves images that it believes are similar to the original image but have different answers to the question. Such explanations can help in building trust for machines among their users.

2. Related Work

Visual Question Answering. A number of recent works have proposed visual question answering datasets [3, 22, 26, 31, 10, 46, 38, 36] and models [9, 25, 2, 43, 24, 27, 47, 45, 44, 41, 35, 20, 29, 15, 42, 33, 17]. Our work builds on top of the VQA dataset from Antol *et al.* [3], which is one of the most widely used VQA datasets. We reduce the language biases present in this popular dataset, resulting in a dataset that is more balanced and about twice the size of the VQA dataset. We benchmark one ‘baseline’ VQA model [24], one attention-based VQA model [25], and the winning model from the VQA Real Open Ended Challenge 2016 [9] on our balanced VQA dataset, and compare them to a language-only model.

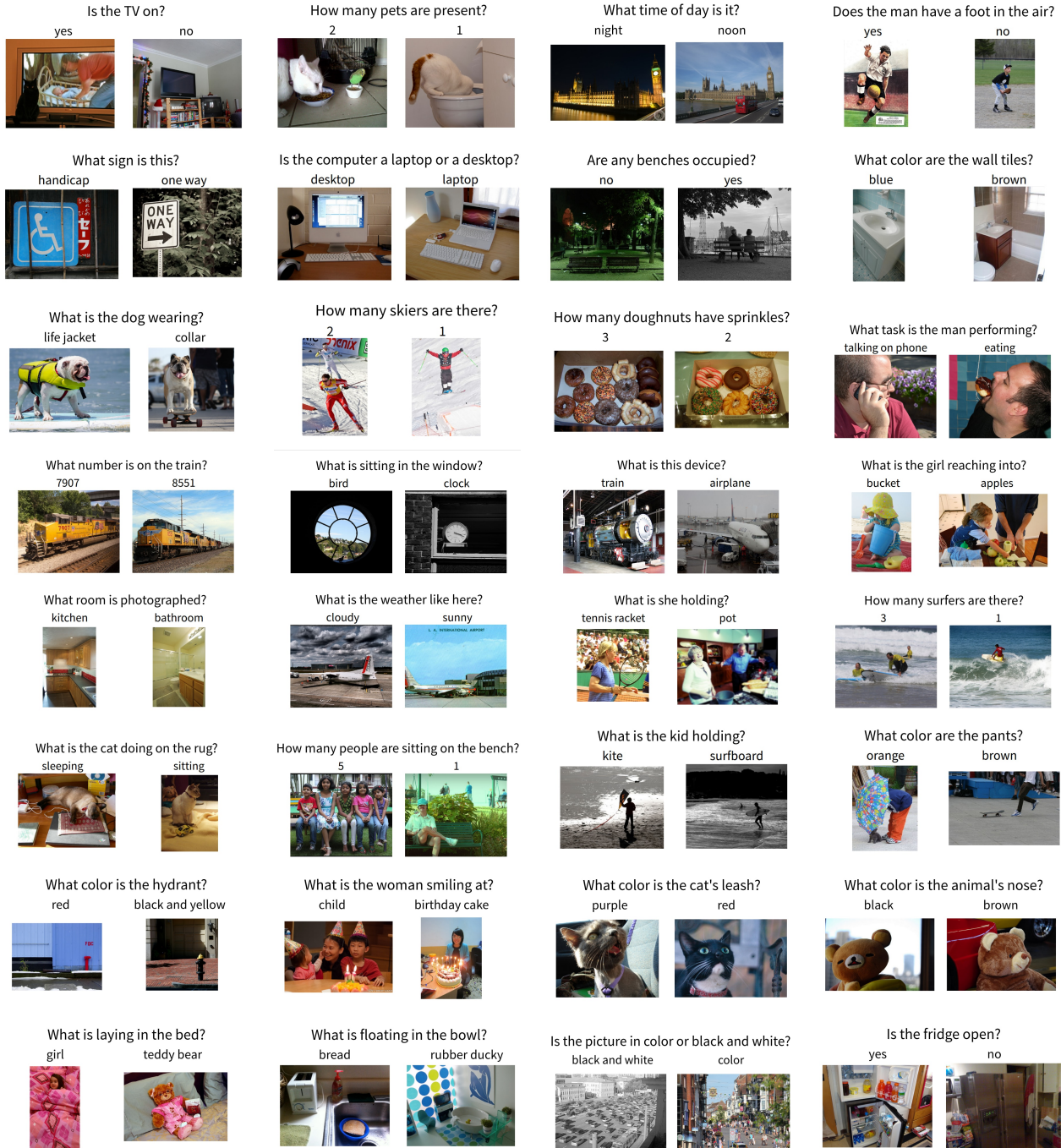


Figure 2: Random examples from our proposed balanced VQA dataset. Each question has two similar images with different answers to the question.

Data Balancing and Augmentation. At a high level, our work may be viewed as constructing a more rigorous evaluation protocol by collecting ‘hard negatives’. In that spirit, it is similar to the work of Hodosh *et al.* [14], who created a binary forced-choice image captioning task, where

a machine must choose to caption an image with one of two similar captions. To compare, Hodosh *et al.* [14] implemented hand-designed rules to create two similar captions for images, while we create a novel annotation interface to collect two similar images for questions in VQA.

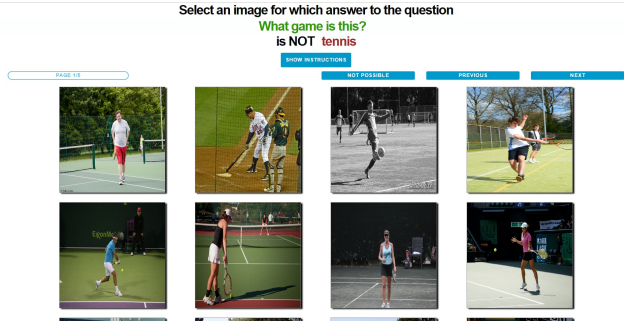


Figure 3: A snapshot of our Amazon Mechanical Turk (AMT) interface to collect complementary images.

Perhaps the most relevant to our work is that of Zhang *et al.* [47], who study this goal of balancing VQA in a fairly restricted setting – binary (yes/no) questions on abstract scenes made from clipart (part of the VQA abstract scenes dataset [3]). Using clipart allows Zhang *et al.* to ask human annotators to “change the clipart scene such that the answer to the question changes”. Unfortunately, such fine-grained editing of image content is simply not possible in real images. The novelty of our work over Zhang *et al.* is the proposed complementary image data collection interface, application to real images, extension to *all* questions (not just binary ones), benchmarking of state-of-art VQA models on the balanced dataset, and finally the novel VQA model with counter-example based explanations.

Models with explanation. A number of recent works have proposed mechanisms for generating ‘explanations’ [13, 34, 48, 11, 32] for the predictions made by deep learning models, which are typically ‘black-box’ and non-interpretable. [13] generates a natural language explanation (sentence) for image categories. [34, 48, 11, 32] provide ‘visual explanations’ or spatial maps overlaid on images to highlight the regions that the model focused on while making its predictions. In this work, we introduce a third explanation modality: counter-examples, instances the the model believes are close to but not belonging to the category predicted by the model.

3. Dataset

We build on top of the VQA dataset introduced by Antol *et al.* [3]. VQA real images dataset contains just over 204K images from COCO [23], 614K free-form natural language questions (3 questions per image), and over 6 million free-form (but concise) answers (10 answers per question). While this dataset has spurred significant progress in VQA domain, as discussed earlier, it has strong language biases.

Our key idea to counter this language bias is the following – for every (image, question, answer) triplet (I, Q, A) in the VQA dataset, our goal is to identify an image I' that

is similar to I , but results in the answer to the question Q to become A' (which is different from A). We built an annotation interface (shown in Fig. 3) to collect such complementary images on Amazon Mechanical Turk (AMT). AMT workers are shown 24 nearest-neighbor images of I , the question Q , and the answer A , and asked to pick an image I' from the list of 24 images for which Q “makes sense” and the answer to Q is *not* A .

To capture “question makes sense”, we explained to the workers (and conducted qualification tests to make sure that they understood) that any premise assumed in the question must hold true for the image they select. For instance, the question “What is the woman doing?” assumes that a woman is present and can be seen in the image. It does not make sense to ask this question on an image without a woman visible in it.

We compute the 24 nearest neighbors by first representing each image with the activations from the penultimate (“fc7”) layer of a deep Convolutional Neural Network (CNN) – in particular VGGNet [37] – and then using ℓ_2 -distances to compute neighbors.

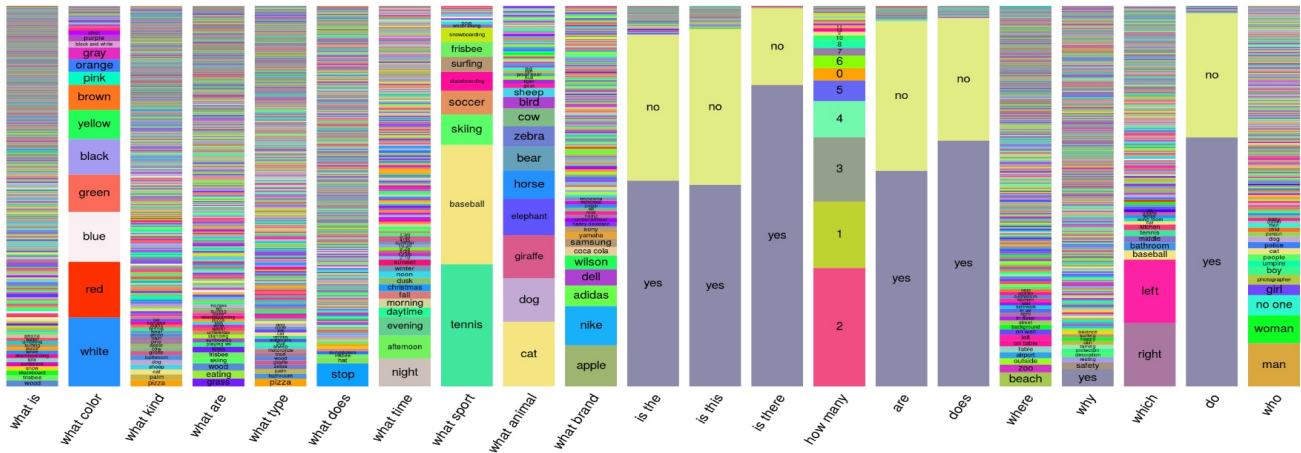
After the complementary images are collected, we conduct a second round of data annotation to collect answers on these new images. Specifically, we show the picked image I' with the question Q to 10 new AMT workers, and collect 10 ground truth answers (similar to [3]). The most common answer among the 10 is the new answer A' .

This two-stage data collection process finally results in pairs of complementary images I and I' that are semantically similar, but have different answers A and A' respectively to the same question Q . Since I and I' are semantically similar, a VQA model will have to understand the subtle differences between I and I' to provide the right answer to both images. Example complementary images are shown in Fig. 1, Fig. 2, and on the project website.

Note that sometimes it may not be *possible* to pick one of the 24 neighbors as a complementary image. This is because either (1) the question does not make sense for any of the 24 images (*e.g.* the question is ‘what is the woman doing?’ and none of the neighboring images contain a woman), or (2) the question is applicable to some neighboring images, but the answer to the question is still A (same as the original image I). In such cases, our data collection interface allowed AMT workers to select “not possible”.

We analyzed the data annotated with “not possible” selection by AMT workers and found that this typically happens when (1) the object being talked about in the question is too small in the original image and thus the nearest neighbor images, while globally similar, do not necessarily contain the object resulting in the question not making sense, or (2) when the concept in the question is rare (*e.g.*, when workers are asked to pick an image such that the answer to the question “What color is the banana?” is NOT “yellow”).

Answers from unbalanced dataset



Answers from balanced dataset

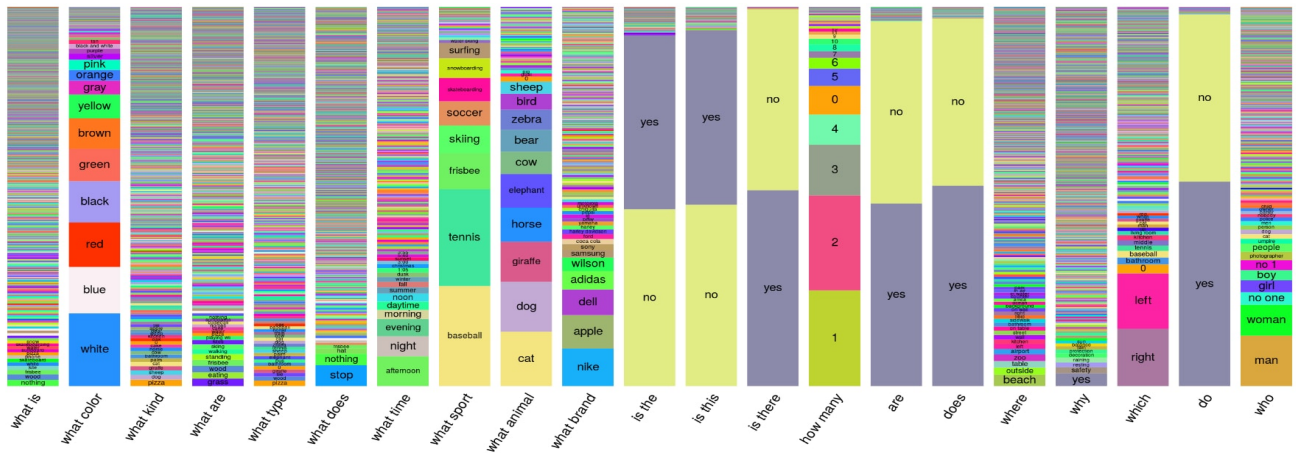


Figure 4: Distribution of answers per question type for a random sample of 60K questions from the original (unbalanced) VQA dataset [3] (top) and from our proposed balanced dataset (bottom).

In total, such “not possible” selections make up 22% of all the questions in the VQA dataset. We believe that a more sophisticated interface that allowed workers to scroll through many more than 24 neighboring images could possibly reduce this fraction. But, (1) it will likely still not be 0 (there may be no image in COCO where the answer to “is the woman flying?” is NOT “no”), and (2) the task would be significantly more cumbersome for workers, making the data collection significantly more expensive.

We collected complementary images and the corresponding new answers for all of train, val and test splits of the VQA dataset. AMT workers picked “not possible” for approximately 135K total questions. In total, we collected approximately 195K complementary images for train, 93K complementary images for val, and 191K complementary images for test set. In addition, we augment the test set with ~18K additional (question, image) pairs to provide

additional means to detect anomalous trends on the test data. Hence, our complete balanced dataset contains more than 443K train, 214K val and 453K test (question, image) pairs. Our complete balanced dataset is publicly available for download.

We use the publicly released VQA evaluation script in our experiments. The evaluation metric uses 10 ground-truth answers for each question to compute VQA accuracies. As described above, we collected 10 answers for every complementary image and its corresponding question to be consistent with the VQA dataset [3]. Note that while unlikely, it is possible that the majority vote of the 10 new answers may not match the intended answer of the person picking the image either due to inter-human disagreement, or if the worker selecting the complementary image simply made a mistake. We find this to be the case – *i.e.*, A to be the same as A' – for about 9% of our questions.

Fig. 4 compares the distribution of answers per question-type in our new balanced VQA dataset with the original (unbalanced) VQA dataset [3]. We notice several interesting trends. First, binary questions (*e.g.* “is the”, “is this”, “is there”, “are”, “does”) have a *significantly* more balanced distribution over “yes” and “no” answers in our balanced dataset compared to unbalanced VQA dataset. “baseball” is now slightly more popular than “tennis” under “what sport”, and more importantly, overall “baseball” and “tennis” dominate less in the answer distribution. Several other sports like “frisbee”, “skiing”, “soccer”, “skateboarding”, “snowboard” and “surfing” are more visible in the answer distribution in the balanced dataset, suggesting that it contains heavier tails. Similar trends can be seen across the board with colors, animals, numbers, *etc.* Quantitatively, we find that the entropy of answer distributions averaged across various question types (weighted by frequency of question types) increases by 56% after balancing, confirming the heavier tails in the answer distribution.

As the statistics show, while our balanced dataset is not perfectly balanced, it is *significantly* more balanced than the original VQA dataset. The resultant impact of this balancing on performance of state-of-the-art VQA models is discussed in the next section.

4. Benchmarking Existing VQA Models

Our first approach to training a VQA model that emphasizes the visual information over language-priors-alone is to re-train the existing state-of-art VQA models (with code publicly available [24, 25, 9]) on our new balanced VQA dataset. Our hypothesis is that simply training a model to answer questions correctly on our balanced dataset will already encourage the model to focus more on the visual signal, since the language signal alone has been impoverished. We experiment with the following models:

Deeper LSTM Question + norm Image (d-LSTM+n-I) [24]: This was the VQA model introduced in [3] together with the dataset. It uses a CNN embedding of the image, a Long-Short Term Memory (LSTM) embedding of the question, combines these two embeddings via a point-wise multiplication, followed by a multi-layer perceptron classifier to predict a probability distribution over 1000 most frequent answers in the training dataset.

Hierarchical Co-attention (HieCoAtt) [25]: This is a recent attention-based VQA model that ‘co-attends’ to both the image and the question to predict an answer. Specifically, it models the question (and consequently the image via the co-attention mechanism) in a hierarchical fashion: at the word-level, phrase-level and entire question-level. These levels are combined recursively to produce a distribution over the 1000 most frequent answers.

Multimodal Compact Bilinear Pooling (MCB) [9]: This is the winning entry on the real images track of the

VQA Challenge 2016. This model uses a multimodal compact bilinear pooling mechanism to attend over image features and combine the attended image features with language features. These combined features are then passed through a fully-connected layer to predict a probability distribution over the 3000 most frequent answers. It should be noted that MCB uses image features from a more powerful CNN architecture ResNet [12] while the previous two models use image features from VGGNet [37].

Baselines: To put the accuracies of these models in perspective, we compare to the following baselines: **Prior:** Predicting the most common answer in the training set, for all test questions. The most common answer is “yes” in both the unbalanced and balanced sets. **Language-only:** This language-only baseline has a similar architecture as Deeper LSTM + Norm I [24] except that it only accepts the question as input and does not utilize any visual information. Comparing VQA models to language-only ablations quantifies to what extent VQA models have succeeded in leveraging the image to answer the questions.

The results are shown in Table 1. For fair comparison of accuracies with original (unbalanced) dataset, we create a balanced train set which is of similar size as original dataset (referred to as B_{half} in table). For benchmarking, we also report results using the full balanced train set.

Approach	UU	UB	$B_{\text{half}}B$	BB
Prior	27.38	24.04	24.04	24.04
Language-only	48.21	41.40	41.47	43.01
d-LSTM+n-I [24]	54.40	47.56	49.23	51.62
HieCoAtt [25]	57.09	50.31	51.88	54.57
MCB [9]	60.36	54.22	56.08	59.14

Table 1: Performance of VQA models when trained/tested on unbalanced/balanced VQA datasets. UB stands for training on Unbalanced train and testing on Balanced val datasets. UU, $B_{\text{half}}B$ and BB are defined analogously.

We see that the current state-of-art VQA models trained on the original (unbalanced) VQA dataset perform significantly worse when evaluated on our balanced dataset, compared to evaluating on the original unbalanced VQA dataset (*i.e.*, comparing UU to UB in the table). This finding confirms our hypothesis that existing models have learned severe language biases present in the dataset, resulting in a reduced ability to answer questions correctly when the same question has different answers on different images. When these models are trained on our balanced dataset, their performance improves (compare UB to $B_{\text{half}}B$ in the table). Further, when models are trained on complete balanced dataset (\sim twice the size of original dataset), the accuracy improves by 2-3% (compare $B_{\text{half}}B$ to BB). This increase

in accuracy suggests that current VQA models are data starved, and would benefit from even larger VQA datasets.

As the absolute numbers in the table suggest, there is significant room for improvement in building visual understanding models that can extract detailed information from images and leverage this information to answer free-form natural language questions about images accurately. As expected from the construction of this balanced dataset, the question-only approach performs *significantly* worse on the balanced dataset compared to the unbalanced dataset, again confirming the language-bias in the original VQA dataset, and its successful alleviation (though not elimination) in our proposed balanced dataset.

Note that in addition to the lack of language bias, visual reasoning is also challenging on the balanced dataset since there are pairs of images very similar to each other in image representations learned by CNNs, but with different answers to the same question. To be successful, VQA models need to understand the subtle differences in these images.

The paired construction of our dataset allows us to analyze the performance of VQA models in unique ways. Given the prediction of a VQA model, we can count the number of questions where *both* complementary images (I, I') received correct answer predictions for the corresponding question Q , or both received identical (correct or incorrect) answer predictions, or both received different answer predictions. For the HieCoAtt [25] model, when trained on the unbalanced dataset, 13.5% of the pairs were answered correctly, 59.9% of the pairs had identical predictions, and 40.1% of the pairs had different predictions. In comparison, when trained on balanced dataset, the same model answered 17.7% of the pairs correctly, a 4.2% increase in performance! Moreover, it predicts identical answers for 10.5% fewer pairs (49.4%). This shows that by training on balanced dataset, this VQA model has learned to tell the difference between two otherwise similar images. However, significant room for improvement remains. The VQA model still can not tell the difference between two images that have a noticeable difference – a difference enough to result in the two images having different ground truth answers for the same question asked by humans.

Analysis of Accuracies for Different Answer Types:

We further analyze the accuracy breakdown over answer types for Multimodal Compact Bilinear Pooling (MCB) [9] and Hierarchical Co-attention (HieCoAtt) [25] models.

The results are shown in Table 2. First, we immediately notice that the accuracy for the answer-type “yes/no” drops significantly from UU to UB ($\sim 10.8\%$ for MCB and $\sim 12.4\%$ for HieCoAtt). This suggests that these VQA models are really exploiting language biases for “yes/no” type questions, which leads to high accuracy on unbalanced val set because the unbalanced val set also contains these biases. But performance drops significantly when tested on

Approach	Ans Type	UU	UB	B _{half} B	BB
MCB [9]	Yes/No	81.20	70.40	74.89	77.37
	Number	34.80	31.61	34.69	36.66
	Other	51.19	47.90	47.43	51.23
	All	60.36	54.22	56.08	59.14
HieCoAtt [25]	Yes/No	79.99	67.62	70.93	71.80
	Number	34.83	32.12	34.07	36.53
	Other	45.55	41.96	42.11	46.25
	All	57.09	50.31	51.88	54.57

Table 2: Accuracy breakdown over answer types achieved by MCB [9] and HieCoAtt [25] models when trained/tested on unbalanced/balanced VQA datasets. UB stands for training on Unbalanced train and testing on Balanced val datasets. UU, B_{half}B and BB are defined analogously.

the balanced val set which has significantly reduced biases.

Second, we note that for both the state-of-art VQA models, the largest source of improvement from UB to B_{half}B is the “yes/no” answer-type ($\sim 4.5\%$ for MCB and $\sim 3\%$ for HieCoAtt) and the “number” answer-type ($\sim 3\%$ for MCB and $\sim 2\%$ for HieCoAtt).

This trend is particularly interesting since the “yes/no” and “number” answer-types are the ones where existing approaches have shown minimal improvements. For instance, in the results announced at the VQA Real Open Ended Challenge 2016², the accuracy gap between the top-4 approaches is a mere 0.15% in “yes/no” answer-type category (and a gap of 3.48% among the top-10 approaches). Similarly, “number” answer-type accuracies only vary by 1.51% and 2.64% respectively. The primary differences between current generation of state-of-art approaches seem to come from the “other” answer-type where accuracies vary by 7.03% and 10.58% among the top-4 and top-10 entries.

This finding suggests that language priors present in the unbalanced VQA dataset (particularly in the “yes/no” and “number” answer-type questions) lead to similar accuracies for all state-of-art VQA models, rendering vastly different models virtually indistinguishable from each other (in terms of their accuracies for these answer-types). Benchmarking these different VQA models on our balanced dataset (with reduced language priors) may finally allow us to distinguish between ‘good’ models (ones that encode the ‘right’ inductive biases for this task, such as attention-based or compositional models) from others that are simply high-capacity models tuning themselves to the biases in the dataset.

²<http://visualqa.org/challenge.html>

5. Counter-example Explanations

We propose a new explanation modality: counter-examples. We propose a model that when asked a question about an image, not only provides an answer, but also provides example images that are similar to the input image but the model believes have different answers to the input question. This would instill trust in the user that the model does in fact ‘understand’ the concept being asked about. For instance, for a question “What color is the fire-hydrant?” a VQA model may be perceived as more trustworthy if in addition to saying “red”, it also adds “unlike this” and shows an example image containing a fire-hydrant that is not red.³

5.1. Model

Concretely, at test time, our “negative explanation” or “counter-example explanation” model functions in two steps. In the first step, similar to a conventional VQA model, it takes in an (image, question) pair (Q, I) as input and predicts an answer A_{pred} . In the second step, it uses this predicted answer A_{pred} along with the question Q to retrieve an image that is similar to I but has a different answer than A_{pred} to the question Q . To ensure similarity, the model picks one of K nearest neighbor images of I , $I_{NN} = \{I_1, I_2, \dots, I_K\}$ as the counter-example.

How may we find these “negative explanations”? One way of picking the counter-example from I_{NN} is to follow the classical “hard negative mining” strategy popular in computer vision. Specifically, simply pick the image that has the lowest $P(A_{pred}|Q, I_i)$ where $i \in 1, 2, \dots, K$. We compare to this strong baseline. While this ensures that $P(A_{pred}|Q, I_i)$ is low for I_i , it does not ensure that the Q “makes sense” for I_i . Thus, when trying to find a negative explanation for “Q: What is the woman doing? A: Playing tennis”, this “hard negative mining” strategy might pick an image without a woman in it, which would make for a confusing and non-meaningful explanation to show to a user, if the goal is to convince them that the model has understood the question. One could add a component of question relevance [30] to identify better counter-examples.

Instead, we take advantage of our balanced data collection mechanism to directly train for identifying a good counter-example. Note that the I' picked by humans is a good counter-example, by definition. Q is relevant to I' (since workers were asked to ensure it was), I' has a different answer A' than A (the original answer), and I' is similar to I . Thus, we have supervised training data where I' is a counter-example from I_{NN} ($K = 24$) for question Q and answer A . We train a model that learns to provide negative or counter-example explanations from this supervised data.

To summarize, during test time, our model does two

³It could easily also convey what color it thinks the fire-hydrant is in the counter-example. We will explore this in future work.

things: first it answers the question (similar to a conventional VQA model), and second, it explains its answer via a counter-example. For the first step, it is given as input an image I and a question Q , and it outputs a predicted answer A_{pred} . For the second (explaining) step, it is given as input the question Q , an answer to be explained A ⁴, and a set I_{NN} from which the model has to identify the counter-example. At training time, the model is given image I , the question Q , and the corresponding ground-truth answer A to learn to answer questions. It is also given Q , A , I' (human-picked), I_{NN} ($I' \in I_{NN}$) to learn to explain.

Our model architecture contains two heads on top of a shared base ‘trunk’ – one head for answering the question and the other head for providing an explanation. Specifically, our model consists of three major components:

1. Shared base: The first component of our model is learning representations of images and questions. It is a 2-channel network that takes in an image CNN embedding as input in one branch, question LSTM embedding as input in another branch, and combines the two embeddings by a point-wise multiplication. This gives us a joint QI embedding, similar to the model in [24]. The second and third components – the answering model and the explaining model – take in this joint QI embedding as input, and therefore can be considered as two heads over this first shared component. A total of 25 images – the original image I and 24 candidate images $\{I_1, I_2, \dots, I_{24}\}$ are passed through this shared component of the network.

2. Answering head: The second component is learning to answer questions. Similar to [24], it consists of a fully-connected layer fed into a softmax that predicts the probability distribution over answers given the QI embedding. Only the QI embedding corresponding to the original image I is passed through this component and result in a cross-entropy loss.

3. Explaining head: The third component is learning to explain an answer A via a counter-example image. It is a 2-channel network which linearly transforms the joint QI embedding (output from the first component) and the answer to be explained A (provided as input)⁵ into a common

⁴In practice, this answer to be explained would be the answer predicted by the first step A_{pred} . However, we only have access to negative explanation annotations from humans for the ground-truth answer A to the question. Providing A to the explanation module also helps in evaluating the two steps of answering and explaining separately.

⁵Note that in theory, one could provide A_{pred} as input during training instead of A . After all, this matches the expected use case scenario at test time. However, this alternate setup (where A_{pred} is provided as input instead of A) leads to a peculiar and unnatural explanation training goal – specifically, the explanation head will *still be* learning to explain A since that is the answer for which we collected negative explanation human annotations. It is simply unnatural to build that model that answers a question with A_{pred} but learn to explain a different answer A ! Note that this is an interesting scenario where the current push towards “end-to-end” training



Figure 5: Three counter-example or negative explanations (right three columns) generated by our model, along with the input image (left), the input question Q and the predicted answer A .

embedding space. It computes an inner product of these 2 embeddings resulting in a scalar number for each image in I_{NN} (also provided as input, from which a counter-example is to be picked). These K inner-product values for K candidate images are then passed through a fully connected layer to generate K scores $S(I_i)$, where $i \in \{1, 2, \dots, K\}$. The K candidate images $\{I_1, I_2, \dots, I_K\}$ are then sorted according to these scores $S(I_i)$ as being most to least likely of being good counter-examples or negative explanations. This component is trained with pairwise hinge ranking losses that encourage $S(I') - S(I_i) > M - \epsilon$, $I_i \in \{I_1, I_2, \dots, I_K\} \setminus \{I'\}$, *i.e.* the score of the human picked image I' is encouraged to be higher than all other candidate images by a desired margin of M (a hyperparameter) and a slack of ϵ . This is of course the classical ‘constraint form’ of the pairwise hinge ranking loss, and we minimize the standard expression $\max(0, M - (S(I') - S(I_i)))$. The combined loss function for the shared component is

$$\mathcal{L} = -\log P(A|I, Q) + \lambda \sum_i \max(0, M - (S(I') - S(I_i))) \quad (1)$$

where, the first term is the cross-entropy loss (for training the answering module) on (I, Q) , the second term is the sum of pairwise hinge losses that encourage the explaining model to give high score to image I' (picked by humans) than other I_i s in I_{NN} , and λ is the trade-off weight parameter between the two losses.

5.2. Results

Fig. 5 shows qualitative examples of negative explanations produced by our model. We see the original image I , the question asked Q , the answer A_{pred} predicted by the VQA head in our model, and top three negative explanations produced by the explanation head. We see that most of these explanations are sensible and reasonable – the images are similar to I but with answers that are different from those predicted for I .

for everything breaks down.

For quantitative evaluation, we compare our model with a number of baselines: **Random**: Sorting the candidate images in I_{NN} randomly. That is, a random image from I_{NN} is picked as the most likely counter-example. **Distance**: Sorting the candidate images in increasing order of their distance from the original image I . That is, the image from I_{NN} most similar to I is picked as the most likely counter-example. **VQA Model**: Using a VQA model’s probability for the predicted answer to sort the candidate images in *ascending* order of $P(A|Q, I_i)$. That is, the image from I_{NN} *least likely* to have A as the answer to Q is picked as the *most likely* counter-example.

Note that while I' – the image picked by humans – is a good counter-example, it is not necessarily the unique (or even the “best”) counter-example. Humans were simply asked to pick any image where Q makes sense and the answer is not A . There was no natural criteria to convey to humans to pick the “best” one – it is not clear what “best” would mean in the first place. To provide robustness to this potential ambiguity in the counter-example chosen by humans, in a manner similar to the ImageNet [5] top-5 evaluation metric, we evaluate our approach using the Recall@5 metric. It measures how often the human picked I' is among the top-5 in the sorted list of I_i s in I_{NN} our model produces.

	Random	Distance	VQA [3]	Ours
Recall@5	20.79	42.84	21.65	43.39

Table 3: Negative or counter-example explanation performance of our model compared to strong baselines.

In Table 3, we can see that our explanation model significantly outperforms the random baseline, as well as the VQA [3] model. Interestingly, the strongest baseline is Distance. While our approach outperforms it, it is clear that identifying an image that is a counter-example to I from among I ’s nearest neighbors is a challenging task. Again, this suggests that visual understanding models that can extract meaningful details from images still remain elusive.

6. Conclusion

To summarize, in this paper we address the strong language priors for the task of Visual Question Answering and elevate the role of image understanding required to be successful on this task. We develop a novel data-collection interface to ‘balance’ the popular VQA dataset [3] by collecting ‘complementary’ images. For every question in the dataset, we have two complementary images that look similar, but have different answers to the question.

This effort results in a dataset that is not only more balanced than the original VQA dataset by construction, but

also is about twice the size. We find both qualitatively and quantitatively that the ‘tails’ of the answer distribution are heavier in this balanced dataset, which reduces the strong language priors that may be exploited by models. Our complete balanced dataset is publicly available at <http://visualqa.org/> as part of the 2nd iteration of the Visual Question Answering Dataset and Challenge (VQA v2.0).

We benchmark a number of (near) state-of-art VQA models on our balanced dataset and find that testing them on this balanced dataset results in a significant drop in performance, confirming our hypothesis that these models had indeed exploited language biases.

Finally, our framework around complementary images enables us to develop a novel explainable model – when asked a question about an image, our model not only returns an answer, but also produces a list of similar images that it considers ‘counter-examples’, *i.e.* where the answer is not the same as the predicted response. Producing such explanations may enable a user to build a better mental model of what the system considers a response to mean, and ultimately build trust.

Acknowledgements. We thank Anitha Kannan and Aishwarya Agrawal for helpful discussions. This work was funded in part by NSF CAREER awards to DP and DB, an ONR YIP award to DP, ONR Grant N00014-14-1-0679 to DB, a Sloan Fellowship to DP, ARO YIP awards to DB and DP, an Allen Distinguished Investigator award to DP from the Paul G. Allen Family Foundation, ICTAS Junior Faculty awards to DB and DP, Google Faculty Research Awards to DP and DB, Amazon Academic Research Awards to DP and DB, AWS in Education Research grant to DB, and NVIDIA GPU donations to DB. The views and conclusions contained herein are those of the authors and should not be interpreted as necessarily representing the official policies or endorsements, either expressed or implied, of the U.S. Government, or any sponsor.

References

- [1] A. Agrawal, D. Batra, and D. Parikh. Analyzing the Behavior of Visual Question Answering Models. In *EMNLP*, 2016. 1
- [2] J. Andreas, M. Rohrbach, T. Darrell, and D. Klein. Deep compositional question answering with neural module networks. In *CVPR*, 2016. 2
- [3] S. Antol, A. Agrawal, J. Lu, M. Mitchell, D. Batra, C. L. Zitnick, and D. Parikh. VQA: Visual Question Answering. In *ICCV*, 2015. 1, 2, 4, 5, 6, 9
- [4] X. Chen and C. L. Zitnick. Mind’s Eye: A Recurrent Visual Representation for Image Caption Generation. In *CVPR*, 2015. 1
- [5] J. Deng, W. Dong, R. Socher, L.-J. Li, K. Li, and L. Fei-Fei. ImageNet: A Large-Scale Hierarchical Image Database. In *CVPR*, 2009. 9
- [6] J. Devlin, S. Gupta, R. B. Girshick, M. Mitchell, and C. L. Zitnick. Exploring nearest neighbor approaches for image captioning. *CoRR*, abs/1505.04467, 2015. 1
- [7] J. Donahue, L. A. Hendricks, S. Guadarrama, M. Rohrbach, S. Venugopalan, K. Saenko, and T. Darrell. Long-term Recurrent Convolutional Networks for Visual Recognition and Description. In *CVPR*, 2015. 1
- [8] H. Fang, S. Gupta, F. N. Iandola, R. Srivastava, L. Deng, P. Dollár, J. Gao, X. He, M. Mitchell, J. C. Platt, C. L. Zitnick, and G. Zweig. From Captions to Visual Concepts and Back. In *CVPR*, 2015. 1
- [9] A. Fukui, D. H. Park, D. Yang, A. Rohrbach, T. Darrell, and M. Rohrbach. Multimodal Compact Bilinear Pooling for Visual Question Answering and Visual Grounding. In *EMNLP*, 2016. 2, 6, 7
- [10] H. Gao, J. Mao, J. Zhou, Z. Huang, and A. Yuille. Are you talking to a machine? dataset and methods for multilingual image question answering. In *NIPS*, 2015. 1, 2
- [11] Y. Goyal, A. Mohapatra, D. Parikh, and D. Batra. Towards Transparent AI Systems: Interpreting Visual Question Answering Models. In *ICML Workshop on Visualization for Deep Learning*, 2016. 4
- [12] K. He, X. Zhang, S. Ren, and J. Sun. Deep residual learning for image recognition. In *CVPR*, 2016. 6
- [13] L. A. Hendricks, Z. Akata, M. Rohrbach, J. Donahue, B. Schiele, and T. Darrell. Generating visual explanations. In *ECCV*, 2016. 4
- [14] M. Hodosh and J. Hockenmaier. Focused evaluation for image description with binary forced-choice tasks. In *Workshop on Vision and Language, Annual Meeting of the Association for Computational Linguistics*, 2016. 3
- [15] I. Ilievski, S. Yan, and J. Feng. A focused dynamic attention model for visual question answering. *CoRR*, abs/1604.01485, 2016. 2
- [16] A. Jabri, A. Joulin, and L. van der Maaten. Revisiting Visual Question Answering Baselines. In *ECCV*, 2016. 1
- [17] K. Kafle and C. Kanan. Answer-type prediction for visual question answering. In *CVPR*, 2016. 2
- [18] K. Kafle and C. Kanan. Visual Question Answering: Datasets, Algorithms, and Future Challenges. *CoRR*, abs/1610.01465, 2016. 1
- [19] A. Karpathy and L. Fei-Fei. Deep Visual-Semantic Alignments for Generating Image Descriptions. In *CVPR*, 2015. 1
- [20] J.-H. Kim, S.-W. Lee, D.-H. Kwak, M.-O. Heo, J. Kim, J.-W. Ha, and B.-T. Zhang. Multimodal Residual Learning for Visual QA. In *NIPS*, 2016. 2
- [21] R. Kiros, R. Salakhutdinov, and R. S. Zemel. Unifying Visual-Semantic Embeddings with Multimodal Neural Language Models. *TACL*, 2015. 1
- [22] R. Krishna, Y. Zhu, O. Groth, J. Johnson, K. Hata, J. Kravitz, S. Chen, Y. Kalantidis, L.-J. Li, D. A. Shamma, et al. Visual genome: Connecting language and vision using crowdsourced dense image annotations. *arXiv preprint arXiv:1602.07332*, 2016. 2
- [23] T.-Y. Lin, M. Maire, S. Belongie, J. Hays, P. Perona, D. Ramanan, P. Dollár, and C. L. Zitnick. Microsoft COCO: Common Objects in Context. In *ECCV*, 2014. 2, 4

- [24] J. Lu, X. Lin, D. Batra, and D. Parikh. Deeper LSTM and normalized CNN Visual Question Answering model. https://github.com/VT-vision-lab/VQA_LSTM_CNN, 2015. 2, 6, 8
- [25] J. Lu, J. Yang, D. Batra, and D. Parikh. Hierarchical Question-Image Co-Attention for Visual Question Answering. In *NIPS*, 2016. 2, 6, 7
- [26] M. Malinowski and M. Fritz. A Multi-World Approach to Question Answering about Real-World Scenes based on Uncertain Input. In *NIPS*, 2014. 1, 2
- [27] M. Malinowski, M. Rohrbach, and M. Fritz. Ask your neurons: A neural-based approach to answering questions about images. In *ICCV*, 2015. 1, 2
- [28] J. Mao, W. Xu, Y. Yang, J. Wang, and A. L. Yuille. Explain Images with Multimodal Recurrent Neural Networks. In *NIPS*, 2014. 1
- [29] H. Noh and B. Han. Training recurrent answering units with joint loss minimization for vqa. *CoRR*, abs/1606.03647, 2016. 2
- [30] A. Ray, G. Christie, M. Bansal, D. Batra, and D. Parikh. Question Relevance in VQA: Identifying Non-Visual And False-Premise Questions. In *EMNLP*, 2016. 8
- [31] M. Ren, R. Kiros, and R. Zemel. Exploring models and data for image question answering. In *NIPS*, 2015. 1, 2
- [32] M. T. Ribeiro, S. Singh, and C. Guestrin. "Why Should I Trust You?": Explaining the Predictions of Any Classifier. In *Knowledge Discovery and Data Mining (KDD)*, 2016. 4
- [33] K. Saito, A. Shin, Y. Ushiku, and T. Harada. Dualnet: Domain-invariant network for visual question answering. *CoRR*, abs/1606.06108, 2016. 2
- [34] R. R. Selvaraju, A. Das, R. Vedantam, M. Cogswell, D. Parikh, and D. Batra. Grad-CAM: Why did you say that? Visual Explanations from Deep Networks via Gradient-based Localization. *arXiv preprint arXiv:1610.02391*, 2016. 4
- [35] K. J. Shih, S. Singh, and D. Hoiem. Where to look: Focus regions for visual question answering. In *CVPR*, 2016. 2
- [36] A. Shin, Y. Ushiku, and T. Harada. The Color of the Cat is Gray: 1 Million Full-Sentences Visual Question Answering (FSVQA). *arXiv preprint arXiv:1609.06657*, 2016. 2
- [37] K. Simonyan and A. Zisserman. Very deep convolutional networks for large-scale image recognition. In *ICLR*, 2015. 2, 4, 6
- [38] M. Tapaswi, Y. Zhu, R. Stiefelhagen, A. Torralba, R. Ur-
tasun, and S. Fidler. MovieQA: Understanding Stories in
Movies through Question-Answering. In *CVPR*, 2016. 2
- [39] A. Torralba and A. Efros. Unbiased look at dataset bias. In *CVPR*, 2011. 2
- [40] O. Vinyals, A. Toshev, S. Bengio, and D. Erhan. Show and Tell: A Neural Image Caption Generator. In *CVPR*, 2015. 1
- [41] P. Wang, Q. Wu, C. Shen, A. van den Hengel, and A. R. Dick. Explicit knowledge-based reasoning for visual question answering. *CoRR*, abs/1511.02570, 2015. 2
- [42] Q. Wu, P. Wang, C. Shen, A. van den Hengel, and A. R. Dick. Ask me anything: Free-form visual question answering based on knowledge from external sources. In *CVPR*, 2016. 2
- [43] C. Xiong, S. Merity, and R. Socher. Dynamic memory networks for visual and textual question answering. In *ICML*, 2016. 2
- [44] H. Xu and K. Saenko. Ask, Attend and Answer: Exploring Question-Guided Spatial Attention for Visual Question Answering. In *ECCV*, 2016. 2
- [45] Z. Yang, X. He, J. Gao, L. Deng, and A. Smola. Stacked Attention Networks for Image Question Answering. In *CVPR*, 2016. 2
- [46] L. Yu, E. Park, A. C. Berg, and T. L. Berg. Visual Madlibs: Fill-in-the-blank Description Generation and Question Answering. In *ICCV*, 2015. 2
- [47] P. Zhang, Y. Goyal, D. Summers-Stay, D. Batra, and D. Parikh. Yin and Yang: Balancing and Answering Binary Visual Questions. In *CVPR*, 2016. 1, 2, 4
- [48] B. Zhou, A. Khosla, A. Lapedriza, A. Oliva, and A. Torralba. Learning Deep Features for Discriminative Localization. In *CVPR*, 2015. 4
- [49] B. Zhou, Y. Tian, S. Sukhbaatar, A. Szlam, and R. Fergus. Simple Baseline for Visual Question Answering. *CoRR*, abs/1512.02167, 2015. 1